THE JOURNAL OF PHYSICAL CHEMISTRY Letters

Letter

pubs.acs.org/JPCL

Carrier Mobility in Graphyne Should Be Even Larger than That in Graphene: A Theoretical Prediction

Jianming Chen,[†] Jinyang Xi,[‡] Dong Wang,*[,‡] and Zhigang Shuai*[,†,‡]

[†]Key Laboratory of Organic Solids, Beijing National Laboratory for Molecular Science (BNLMS), Institute of Chemistry, Chinese Academy of Sciences, 100190 Beijing, People's Republic of China

[‡]MOE Key Laboratory of Organic OptoElectronics and Molecular Engineering, Department of Chemistry, Tsinghua University, 100084 Beijing, People's Republic of China

ABSTRACT: We show here that the carrier mobility in the novel sp−sp^2 hybridization planar 6,6,12-graphyne sheet should be even larger than that in the graphene sheet. Both graphyne and graphene exhibit a Dirac cone structure near the Fermi surface. However, due to the sp−sp^2 hybridization forming the triple bonds in graphyne, the electron−phonon scattering is reduced compared with that of graphene. The carrier mobility is calculated at the first-principles level by using the Boltzmann transport equation coupled with the deformation potential theory. The intrinsic mobility of the 6,6,12-graphyne is 4.29×10^5 cm^2 V^{-1} s^{-1} for holes and 5.41×10^5 cm^2 V^{-1} s^{-1} for electrons at room temperature, which is found to be larger than that of graphene ($\sim 3 \times 10^5$ cm^2 V^{-1} s^{-1}).

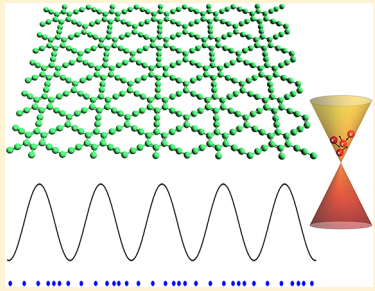

SECTION: Energy Conversion and Storage; Energy and Charge Transport

Graphene as a promising carbon-based electronic material has attracted tremendous interest of research. The exotic electronic properties of graphene originate from its unusual band structure, featuring Dirac points and cones. The linear energy−momentum relationship of graphene causes charge carriers in it to behave as massless Dirac fermions that travel at a speed of 10^6 m s^{-1}.[1] The existence of Dirac cones is also responsible for an anomalous quantum Hall effect[1−3] and high-temperature superconductivity.[4] Dirac cones and their associated transport properties had been considered as a unique feature of graphene related to its hexagonal symmetry until recently; Görling and his colleagues predicted by first-principles band structure calculations that Dirac cones exist in materials other than graphene.[5] The materials that they investigated are a novel type of two-dimensional (2D) carbon allotropes named graphyne, a family of low-energy carbon phases that consist of sp^2 and sp hybridized carbon atoms, which was first proposed by Baughman et al. in 1987.[6] Görling et al.[5] showed that Dirac points and cones not only exist in the α- and β-graphyne with hexagonal symmetry but also in the 6,6,12-graphyne with rectangular symmetry, even in graphynes containing heteroatoms.[7] Their findings revealed that a wealth of 2D materials with various symmetries and chemical compositions could feature Dirac cones and extremely high carrier mobilities and await to be discovered.

So far, only building blocks and cutouts of finite-size graphynes have been synthesized, but experimentalists are taking the very first steps toward the fabrication of extended 2D materials. For instance, a large area ($\sim$3.6 cm^2) of a graphdiyne thin film, which is a carbon allotrope containing diacetylenic linkages, was recently synthesized by Li et al. on top of a copper surface via a cross-linking reaction.[8] The chemical vapor deposition of organic precursor molecules on metal surfaces is anticipated to open a new route to prepare 2D graphyne sheets. Pioneering electronic structure calculations on graphynes and graphdiynes have provided a fundamental understanding toward the sp^2−sp hybridized 2D materials, including the recent discovery of Dirac cones in various types of graphynes ranging from α-, β-, and 6,6,12-graphyne to 6_{BN},6,12- and 6(H_2),14,18-heteroatom graphynes.[7] The existence of Dirac points and cones indicates that intrinsic carrier mobilities in these 2D materials could be as high as those of graphene. Inspired by the new discovery, in this work, we predict intrinsic carrier mobilities of graphynes based on first-principles band structure calculations and the Boltzmann transport theory[9] under the deformation potential (DP) approximation.[10] The theories and computational scheme have been applied successfully to predicting intrinsic carrier mobilities of graphene, which yields comparable mobilities of holes and electrons as high as 10^5 cm^2 V^{-1} s^{-1} at 300 K[11] in reasonable agreement with the experimentally measured values of $2-25 \times 10^4$ cm^2 V^{-1} s^{-1}.[12−16] Most strikingly, we showed that the polarity of the transport, that is, whether it is hole or electron transport, can be tuned by nanoengineering the width of graphene ribbons. The theories and first-principles calculations also predicted that graphdiyne is a semiconductor with electron mobility comparable to, and hole mobility one order of magnitude lower than, that of graphene.[17] It is then asked whether there exist materials whose intrinsic carrier mobilities are higher than those of graphene. Our answer to this question

Received: March 11, 2013
Accepted: April 7, 2013
Published: April 7, 2013

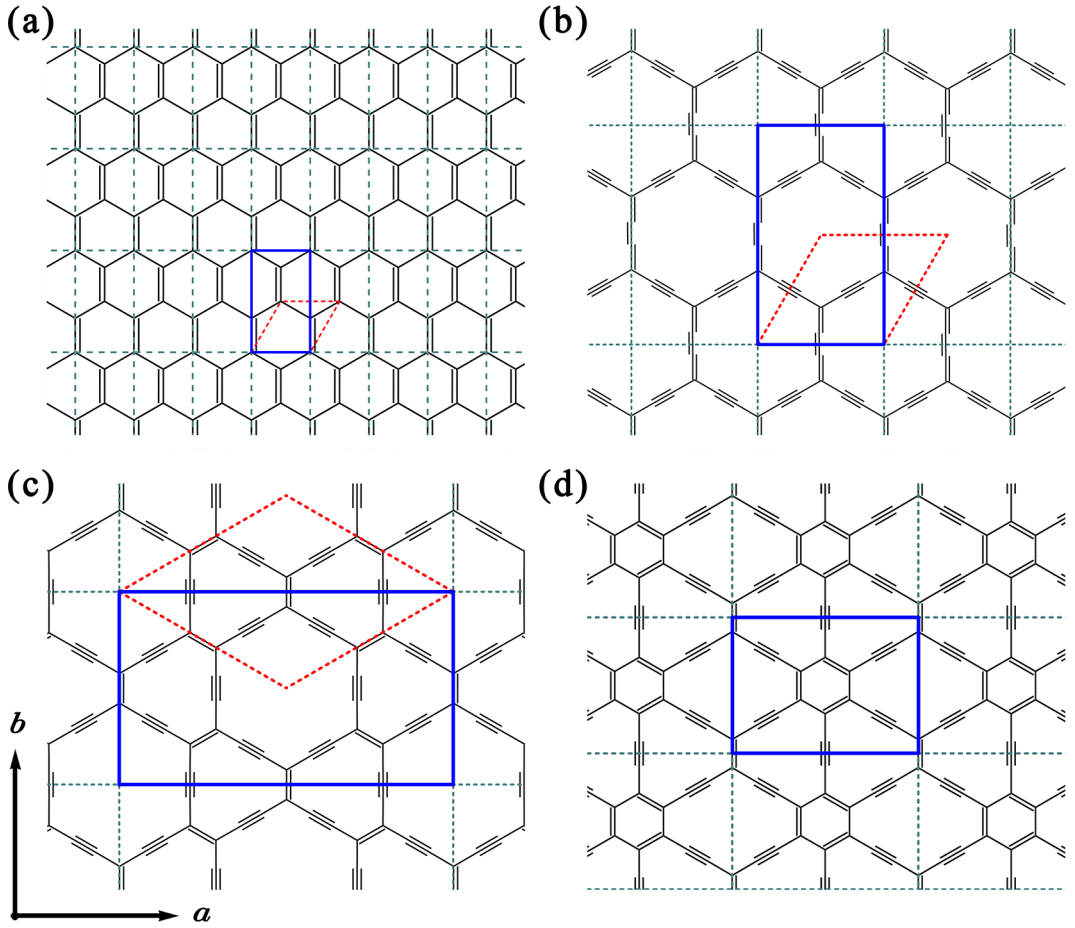

Figure 1. Schematic representation of (a) graphene, (b) α-graphyne, (c) β-graphyne, and (d) 6,6,12-graphyne lattices. For the α- and β-graphynes, both the rhombus primitive cell (red dotted lines) and the rectangular supercell (blue solid lines) are labeled. The latter is used for the DP calculation. For the 6,6,12-graphyne, the primitive cell is rectangular. The a and b directions are oriented along the zigzag and armchair edges of graphene and graphyne.

is positive, and we find in this work that carrier mobilities in the 6,6,12-graphyne could be even larger than those of graphene.

As shown in Figure 1, the α- and β-graphynes are of hexagonal symmetry like graphene, whereas the 6,6,12-graphyne is of rectangular symmetry. These graphynes differ from each other in the percentage of acetylenic linkage in their structures. For the α-graphyne, all of the sp^2 bonds in graphene have been replaced by the acetylenic linkages. The percentage of the acetylenic linkages is 66.67% for the β-graphyne and 41.67% for the 6,6,12-graphyne. Using graphene as the reference, zigzag and armchair edges are oriented along the a and b directions, respectively. We performed the first-principles band structure calculations with the Vienna ab initio package (VASP)[18,19] using the projector augmented wave method and the Perdew–Burke–Ernzerhof (PBE) functional.[20] Optimization of the lattice vectors and atomic positions with a $31 \times 31 \times 1$ Monkhorst–Pack **k**-mesh[21] and an energy cutoff of 600 eV yields the lattice constants of a = 9.44 Å and b = 6.90 Å for the 6,6,12-graphyne. The a and b directions are defined as oriented along the zigzag and armchair edges of graphene and graphyne.

The band structures and density of states (DOS) of the α-, β-, and 6,6,12-graphynes are shown in Figure 2. The 2D contour plots of the valence band (VB) and conduction band (CB) energies in the reciprocal space are displayed in Figure 3 to clearly demonstrate the location and shape of the Dirac cones. There exist two and six Dirac points, respectively, in the first Brillouin zone of the α- and β-graphyne. The two and six points are related by symmetry, as can be seen from Figure 3. For the α-graphyne, the Dirac point is located at the high-symmetry K-point in the irreducible Brillouin zone, similar to that of graphene. Consequently, the Dirac cones exhibit a three-fold symmetry. In the β-graphene, the Dirac point is located on the line from Γ to M, and the Dirac cones exhibit a reflection symmetry with respect to the Γ–M direction. Compared to graphene and the α- and β-graphynes, two pairs of Dirac points have been observed in the first Brillouin zone of the 6,6,12-graphyne. The Dirac points of each pair are symmetry-related. One of the two nonequivalent Dirac points in the irreducible Brillouin zone is along the direction from Γ to X′ (Dirac cone I), and the other is located on the line from M to X near the high-symmetry X-point (Dirac cone II), which is in agreement with Görling's results.[5] The Dirac cones I and II exhibit a reflection symmetry with respect to the mirror line from Γ to X′ and the line from M to X, respectively. Apparently, the slope of Dirac cone I is much larger than that of Dirac cone II. The slopes and curvatures of the Dirac cones are significantly relevant to the intrinsic carrier mobilities.

For a perfect $sp–sp^2$ hybridized 2D graphyne sheet, the charge carriers are delocalized, and the band theory is appropriate for description of the charge transport.[22,23] When the carriers are accelerated in the electric field, they are subject to scatterings by phonons. The Boltzmann transport equation

dx.doi.org/10.1021/jz4005587 | J. Phys. Chem. Lett. 2013, 4, 1443–1448

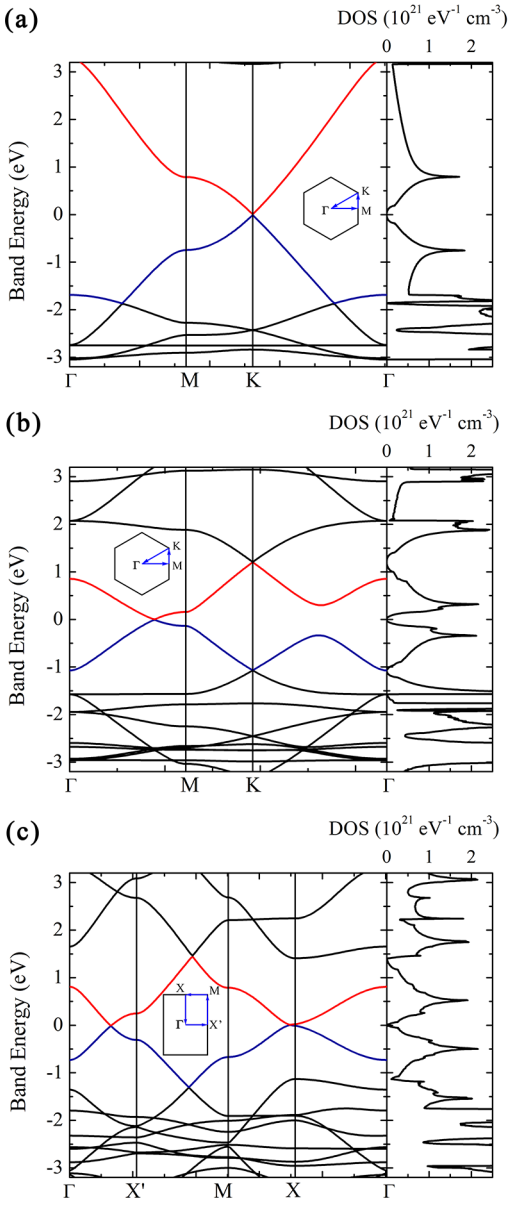

Figure 2. Band structures and DOS of the (a) α-graphyne, (b) β-graphyne, and (c) 6,6,12-graphyne. The Fermi level has been shifted to zero. The Dirac points are located where the CB (red line) bottom and the VB (blue line) top meet.

describes the time evolution of the carrier distribution function and can be solved in the relaxation time approximation. The relaxation times measure how quickly the carriers can restore their equilibrium distribution via scatterings with phonons. The DP theory first proposed by Bardeen and Shockley[10] can be used to describe the electron−acoustic phonon scattering in the long-wave limit. The theory assumes that the local deformations produced by the lattice waves are in analogy to those in the homogeneously deformed lattices. The advantage of the simplified DP theory is that the electron−phonon scattering matrix element can be derived first-principlely. We have successfully applied the DP theory to the calculation of relaxation times and prediction of carrier mobilities of organic molecular crystals[24,25] and carbon-based electronic materials such as graphene and graphdiyne sheets and nanoribbons.[11,17] The relaxation times of carriers due to the electron−acoustic phonon scatterings can be expressed as

$$\frac{1}{\tau_\beta(i,\mathbf{k})} = \frac{2\pi}{\hbar}\frac{k_B T E_1^2}{C}\sum_{\mathbf{k}'\in BZ}\delta[\varepsilon(i,\mathbf{k}') - \varepsilon(i,\mathbf{k})]\left[1 - \frac{v_\beta(i,\mathbf{k}')}{v_\beta(i,\mathbf{k})}\right] \quad (1)$$

where β is the direction of the external field. $\tau(i,\mathbf{k})$, $\varepsilon(i,\mathbf{k})$ and $v(i,\mathbf{k})$ denote the relaxation time, the band energy, and the group velocity at the $\mathbf{k}$-point of the ith band, respectively. E_1 is the DP constant, and C is the 2D elastic constant.

The solution to the Boltzmann transport equation[9] gives the steady-state distribution function of carriers in the external field. The carrier mobility, defined as the drift velocity of charge carriers in the unit electric field, is derived. The Boltzmann transport theory has been proved reliable for carrier transport at the Dirac point for graphene at a relatively low carrier density.[26] In our work, the mobility of holes and electrons is expressed as

$$\mu_\beta^{e(h)} = \frac{e}{k_B T}\frac{\sum_{i\in CB(VB)}\int \tau_\beta(i,\mathbf{k}) v_\beta^2(i,\mathbf{k}) f_0^{e(h)}(\varepsilon)\,d\mathbf{k}}{\sum_{i\in CB(VB)}\int f_0^{e(h)}(\varepsilon)\,d\mathbf{k}} \quad (2)$$

where f_0 is the Fermi−Dirac distribution function expressed as $f_0^e(\varepsilon) = (1 + \exp[(\varepsilon - \varepsilon_F)/k_B T])^{-1}$ and $v_\beta(i,\mathbf{k})$ is the β Cartesian component of the group velocity defined as $v_\beta(i,\mathbf{k}) = (1/\hbar)\cdot\partial\varepsilon(i,\mathbf{k})/\partial k_\beta$.

According to eq 2, to obtain accurate carrier mobilities, we need energy grids on a very fine $\mathbf{k}$-mesh. On the basis of the charge density previously converged on a 31 × 31 × 1 $\mathbf{k}$-mesh, the electronic energies on a 121 × 85 × 1, 41 × 61 × 1 and 71 × 71 × 1 $\mathbf{k}$-mesh, respectively, were calculated from non-self-consistent runs for the α-, β-, and 6,6,12-graphyne. The DP constant E_1 characterizes the coupling strength of the charge carriers with the acoustic phonons. To obtain the DP constant, we dilate the lattice cell up to 1.5% along the a and b axes and measure the shift of the energy band edge. The atomic positions are relaxed upon each dilation. Because the graphyne band features Dirac points and cones, we follow the Fermi level change as a function of dilation. The relationship between the Fermi level position and the dilation $\Delta l/l_0$ is plotted in Figure 4. The DP constant is defined as $E_1 = \Delta E/(\Delta l/l_0)$, where ΔE is the band energy shift. By linearly fitting the data, we obtain the DP constant E_1 for both electrons and holes. With the dilation scheme, we can also obtain the 2D elastic constant C by quadratic fitting of the total energy E with respect to the dilation $\Delta l/l_0$ as $(E - E_0)/S_0 = (C/2)(\Delta l/l_0)^2$; see Figure 4. S_0 is the cell area in the ab plane, and E_0 is the total energy of the cell without dilation. Combining eqs 1 and 2, we finally obtain the relaxation times and the intrinsic mobilities of graphynes. The results are summarized in Tables 1 and 2. The elastic constants, the DP constants, the relaxation times, and the mobilities of graphene and graphdiyne obtained in our previous studies are also provided for comparison.[11,17,25]

It can be seen from Table 1 that the elastic constant of graphyne decreases as the percentage of acetylenic linkages increases. Graphdiyne has a similar atomic geometry as graphene, but all of the sp^2 bonds have been replaced by the diacetylenic linkages. The percentage of the acetylenic linkage is 50% for graphdiyne, and the elastic constant of graphdiyne lies in between those of the 6,6,12- and β-graphyne. The mechanical properties of graphynes have been investigated using molecular dynamics simulations recently.[27] A similar trend has been observed there, with the fracture stress highest

dx.doi.org/10.1021/jz4005587 | J. Phys. Chem. Lett. 2013, 4, 1443−1448

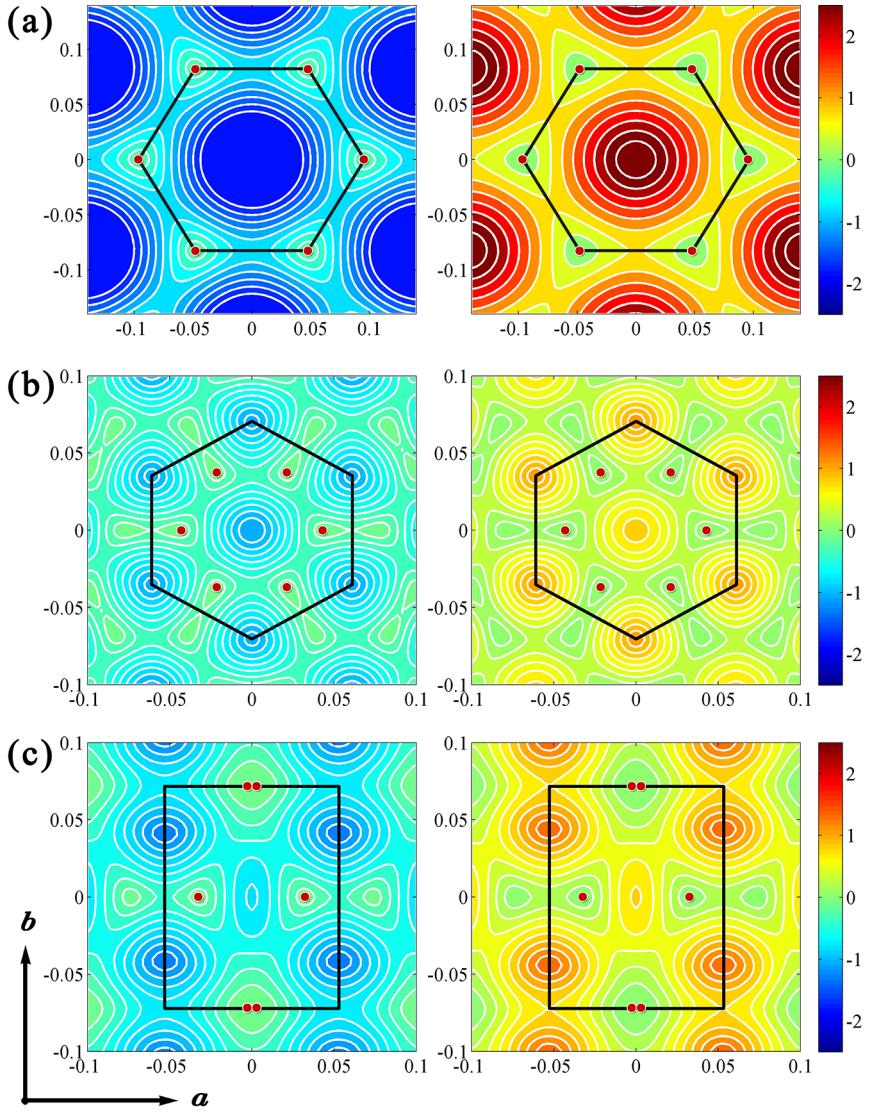

Figure 3. Contour plots of VB and CB energies of the (a) α-graphyne, (b) β-graphyne, and (c) 6,6,12-graphyne in the Brillouin zone. The area surrounded by the black solid lines is the first Brillouin zone. The locations of the Dirac points are highlighted by the red dots.

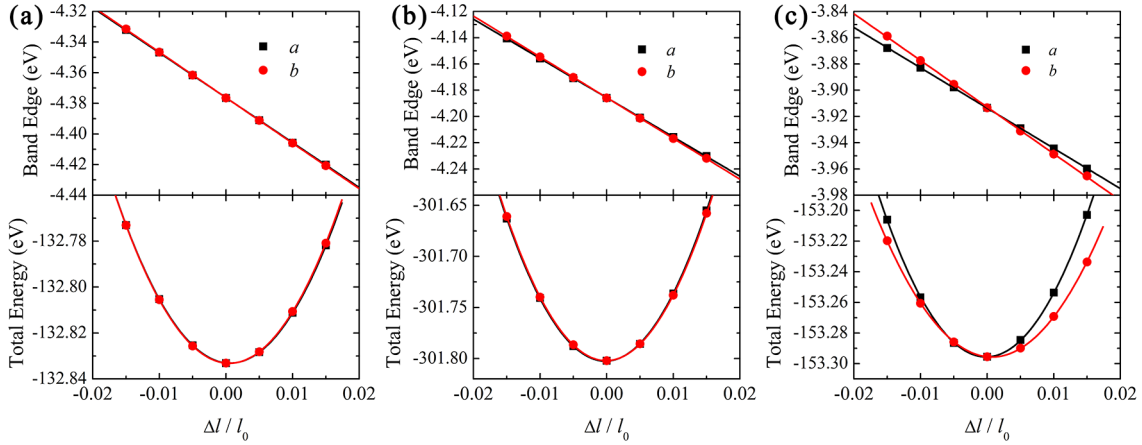

Figure 4. DP constant and 2D elastic constant evaluation for the (a) α-graphyne, (b) β-graphyne, and (c) 6,6,12-graphyne. (Upper) Fermi level shift with respect to the lattice dilation $\Delta l/l_0$. The linear fit of the data gives the DP constant. (Lower) Total energy with respect to the lattice dilation $\Delta l/l_0$. The quadratic fit of the data gives the 2D elastic constant.

in graphene, followed by the γ-, 6,6,12-, β-, and α-graphyne. This can be explained as follows. With the increase in the linkages, the carbon atoms in the structures become sparser, which leads to fewer bond connections and smaller fracture

dx.doi.org/10.1021/jz4005587 | J. Phys. Chem. Lett. 2013, 4, 1443−1448

Table 1. Elastic Constants C and DP Constants E_1 for the α-, β-, and 6,6,12-Graphyne, As Well As Graphene and Graphdiyne

carbon allotropes	acetylenic linkage (%)	axis	C (J m^{-2})	E_1 (eV)
α-graphyne	100	a	94.30	2.94
		b	95.19	2.97
β-graphyne	66.67	a	131.41	2.99
		b	130.65	3.11
6,6,12-graphyne	41.67	a	199.37	3.07
		b	150.52	3.56
graphene	0	a	328.02	5.14
		b	328.30	5.00
graphdiyne	50	a	158.57	6.30 (h)/2.09 (e)
		b	144.90	6.11 (h)/2.19 (e)

stresses. Opposite to the fracture stress, the fracture strain increases with increasing the acetylenic linkages because the presence of the linkages makes graphynes less rigid. Therefore, the Young's modulus decreases with increasing acetylenic linkages. It is further noted from Table 1 that the 6,6,12-graphyne displays a strong anisotropy in the elastic constant. For the other graphynes and graphene, their elastic constants in the a and b directions are rather close, exhibiting little anisotropy. The reason is that all of the graphynes and graphene have hexagonal symmetry except for the 6,6,12-graphyne.

Similar to the elastic constant, the DP constant also decreases with increasing the acetylenic linkages. Graphene possesses the largest DP constant, followed by the 6,6,12-, β-, and α-graphyne. This can be attributed to the fact that the sp triple bonds are stronger than the sp^2 double bonds; therefore, the energies of graphynes are not prone to change upon lattice deformations. The DP constants of the three different graphynes investigated here are found to be close to each other. Graphdiyne is a semiconductor, and its DP constants for electrons and holes are different. The DP constant of graphdiyne for electrons is even smaller than that of graphynes due to the stronger diacetylenic linkages in graphdiyne. It is also observed from Table 1 that the DP constant in the armchair (b) direction is always larger than that in the zigzag (a) direction. This can be explained by the orientation of sp and sp^2 bonds in the structures of graphene, graphynes, and graphdiyne. As shown in Figure 1, there are bonds oriented along the armchair (b) direction, but no bonds are parallel to the zigzag (a) direction. When the lattice deformation is applied in the b direction, the bonds are directly dilated, which can cause a large band energy shift. In contrast, when the deformation is applied in the a direction, the dilation is not in the bond direction, and its influence on the bond length and the corresponding band energy is not as strong as that in the b direction. Therefore, the anisotropy in the DP constant can be attributed to the difference in the bond orientation in the structures. Among the three different graphynes, graphene, and graphdiyne, the 6,6,12-graphyne displays the strongest anisotropy, which is a result of its rectangular symmetry.

The elastic constant and the DP constant together can determine the electron−phonon coupling strength. According to eq 1, the relaxation time is proportional to the elastic constant but inversely proportional to the square of the DP constant. It has been mentioned above that the DP constants of the 6,6,12-, β-, and α-graphyne are rather close; therefore, the relaxation times of the three graphynes are determined mainly by their elastic constants. It can be seen from Table 2 that the relaxation time decreases as the percentage of acetylenic linkages increases from 41.67% for the 6,6,12-graphyne to 100% for the α-graphyne. The largest relaxation time for the 6,6,12-graphyne eventually leads to the highest carrier mobility. It is noted that the relaxation time for electrons in graphdiyne is even larger than that in the 6,6,12-graphyne because graphdiyne has a moderate elastic constant and a much smaller DP constant for electrons, but graphdiyne does not feature the Dirac cones and linear dispersions; as a result, it exhibits a high electron mobility but not as high as that for the 6,6,12-graphyne.

Finally, it comes to the question raised at the beginning of the Letter, are there any materials whose intrinsic carrier mobilities are higher than those of graphene? Compared to graphene, the 6,6,12-graphyne has a smaller elastic constant and a much smaller DP constant in the zigzag (a) direction, which leads to electron−phonon couplings in the 6,6,12-graphyne that are weaker than those in graphene. As a result, the relaxation time for electrons in the 6,6,12-graphyne along the a direction is larger than that in graphene. According to eq 2, the intrinsic carrier mobilities rely on not only the relaxation times but also on the group velocities and the shapes of the Fermi surfaces. The 6,6,12-graphyne features two nonequivalent Dirac cones, and the carriers in it behave like the Dirac fermions traveling at a speed of light, as in graphene. We find that the carrier mobilities of the 6,6,12-graphyne in the a direction are even higher than those of graphene for both electrons and holes. Due to the rectangular symmetry of the 6,6,12-graphyne lattice, its Dirac cones and electron−phonon couplings are

Table 2. Relaxation Times τ and Intrinsic Mobilities μ of Holes and Electrons at 300 K for the α-, β-, and 6,6,12-Graphyne, As Well As Graphene and Graphdiyne

carbon allotropes	axis	τ^h (ps)	τ^e (ps)	μ^h (10^4 cm^2 V^{-1} s^{-1})	μ^e (10^4 cm^2 V^{-1} s^{-1})
α-graphyne	a	2.84	2.83	3.316	3.327
	b	2.80	2.79	2.960	2.716
β-graphyne	a	5.82	6.40	1.076	0.892
	b	5.37	5.91	0.856	0.798
6,6,12-graphyne	a	12.31	17.75	42.92	54.10
	b	6.93	9.99	12.29	24.48
graphene	a	13.80	13.94	32.17	33.89
	b	13.09	13.22	35.12	32.02
graphdiyne	a	1.94	19.11	1.97	20.81
	b	1.88	15.87	1.91	17.22

dx.doi.org/10.1021/jz4005587 | J. Phys. Chem. Lett. 2013, 4, 1443−1448

highly anisotropic, which leads to the anisotropic carrier transport in the 6,6,12-graphyne. In contrast, the carrier transport in graphene is almost isotropic. The directional-dependent carrier transport is anticipated to make the 6,6,12-graphyne more versatile than graphene in potential applications.

To conclude, we employ the Boltzmann transport theory coupled with the DP theory to predict at the first-principles level the intrinsic carrier mobilities for the α-, β-, and 6,6,12-graphynes. Our theoretical results suggest that the 6,6,12-graphyne exhibits a carrier mobility larger than that of graphene in one direction for both electrons and holes. The intrinsic carrier mobility of 6,6,12-graphyne at room temperature can reach 5.41×10^5 and 4.29×10^5 $cm^2 V^{-1} s^{-1}$ for electrons and holes, respectively. The high carrier mobility of 6,6,12-graphyne is a result of weaker electron−phonon coupling strength and longer relaxation times. The rectangular symmetry of the 6,6,12-graphyne lattice is responsible for the anisotropic transport in it. The anisotropic transport that is not found in graphene could be exploited in nanoscale electronic devices. In addition, a strong correlation between the percentage of acetylenic linkages and the elastic constant, the DP constant, and, thereby, the electron−phonon coupling strength, has been revealed for these 2D carbon allotropes. It is found that the hybridization of sp−sp^2 carbon is capable of improving the planar transport behaviors of the carbon allotropes. Focusing on the features of Dirac cones, band structure engineering can provide a clue for tuning the electronic transport in 2D carbon-based materials.

AUTHOR INFORMATION

Corresponding Author

*E-mail: dong913@tsinghua.edu.cn (D.W.); zgshuai@tsinghua.edu.cn (Z.S.).

Notes

The authors declare no competing financial interest.

ACKNOWLEDGMENTS

This work is supported by the National Natural Science Foundation of China (Grants 21273124 and 21290191) and the Ministry of Science and Technology of China (Grants 2011CB932304, 2011CB808405, and 2013CB933503).

REFERENCES

(1) Novoselov, K. S.; Geim, A. K.; Morozov, S. V.; Jiang, D.; Katsnelson, M. I.; Grigorieva, I. V.; Dubonos, S. V.; Firsov, A. A. Two-Dimensional Gas of Massless Dirac Fermions in Graphene. *Nature* **2005**, *438*, 197−200.

(2) Novoselov, K. S.; McCann, E.; Morozov, S. V.; Fal'ko, V. I.; Katsnelson, M. I.; Zeitler, U.; Jiang, D.; Schedin, F.; Geim, A. K. Unconventional Quantum Hall Effect and Berry's Phase of 2π in Bilayer Graphene. *Nat. Phys.* **2006**, *2*, 177−180.

(3) Zhang, Y.; Tan, Y.-W.; Stormer, H. L.; Kim, P. Experimental Observation of the Quantum Hall Effect and Berry's Phase in Graphene. *Nature* **2005**, *438*, 201−204.

(4) Pathak, S.; Shenoy, V. B.; Baskaran, G. Possible High-Temperature Superconducting State with a *d+id* Pairing Symmetry in Doped Graphene. *Phys. Rev. B* **2010**, *81*, 085431.

(5) Malko, D.; Neiss, C.; Viñes, F.; Görling, A. Competition for Graphene: Graphynes with Direction-Dependent Dirac Cones. *Phys. Rev. Lett.* **2012**, *108*, 086804.

(6) Baughman, R. H.; Eckhardt, H.; Kertesz, M. Structure−Property Predictions for New Planar Forms of Carbon: Layered Phases Containing sp^2 and *sp* Atoms. *J. Chem. Phys.* **1987**, *87*, 6687.

(7) Malko, D.; Neiss, C.; Görling, A. Two-Dimensional Materials with Dirac Cones: Graphynes Containing Heteroatoms. *Phys. Rev. B* **2012**, *86*, 045443.

(8) Li, G. X.; Li, Y. L.; Liu, H. B.; Guo, Y. B.; Li, Y. J.; Zhu, D. B. Architecture of Graphdiyne Nanoscale Films. *Chem. Commun.* **2010**, *46*, 3256−3258.

(9) Ziman, J. M. *Principles of the Theory of Solids*; Cambridge: New York, 1964.

(10) Bardeen, J.; Shockley, W. Deformation Potentials and Mobilities in Non-Polar Crystals. *Phys. Rev.* **1950**, *80*, 72.

(11) Long, M. Q.; Tang, L.; Wang, D.; Wang, L. J.; Shuai, Z. G. Theoretical Predictions of Size-Dependent Carrier Mobility and Polarity in Graphene. *J. Am. Chem. Soc.* **2009**, *131*, 17728−17729.

(12) Bolotin, K. I.; Sikes, K. J.; Jiang, Z.; Klima, M.; Fudenberg, G.; Hone, J.; Kim, P.; Stormer, H. L. Ultrahigh Electron Mobility in Suspended Graphene. *Solid State Commun.* **2008**, *146*, 351−355.

(13) Chen, J.-H.; Jang, C.; Xiao, S.; Ishigami, M.; Fuhrer, M. S. Intrinsic and Extrinsic Performance Limits of Graphene Devices on SiO_2. *Nat. Nanotechnol.* **2008**, *3*, 206−209.

(14) Du, X.; Skachko, I.; Barker, A.; Andrei, E. Y. Approaching Ballistic Transport in Suspended Graphene. *Nat. Nanotechnol.* **2008**, *3*, 491−495.

(15) Orlita, M.; Faugeras, C.; Plochocka, P.; Neugebauer, P.; Martinez, G.; Maude, D. K.; Barra, A. L.; Sprinkle, M.; Berger, C.; de Heer, W. A.; et al. Approaching the Dirac Point in High-Mobility Multilayer Epitaxial Graphene. *Phys. Rev. Lett.* **2008**, *101*, 267601.

(16) Tan, Y. W.; Zhang, Y.; Bolotin, K.; Zhao, Y.; Adam, S.; Hwang, E. H.; Das Sarma, S.; Stormer, H. L.; Kim, P. Measurement of Scattering Rate and Minimum Conductivity in Graphene. *Phys. Rev. Lett.* **2007**, *99*, 246803.

(17) Long, M. Q.; Tang, L.; Wang, D.; Li, Y. L.; Shuai, Z. G. Electronic Structure and Carrier Mobility in Graphdiyne Sheet and Nanoribbons: Theoretical Predictions. *ACS Nano* **2011**, *5*, 2593−2600.

(18) Kresse, G.; Furthmüller, J. Efficient Iterative Schemes for *Ab Initio* Total-Energy Calculations Using a Plane-Wave Basis Set. *Phys. Rev. B* **1996**, *54*, 11169−11186.

(19) Kresse, G.; Furthmüller, J. Efficiency of Ab-Initio Total Energy Calculations for Metals and Semiconductors Using a Plane-Wave Basis Set. *Comput. Mater. Sci.* **1996**, *6*, 15−50.

(20) Perdew, J. P.; Burke, K.; Ernzerhof, M. Generalized Gradient Approximation Made Simple. *Phys. Rev. Lett.* **1996**, *77*, 3865−3868.

(21) Monkhorst, H. J.; Pack, J. D. Special Points for Brillouin-Zone Integrations. *Phys. Rev. B* **1976**, *13*, 5188−5192.

(22) Geng, H.; Peng, Q.; Wang, L. J.; Li, H. J.; Liao, Y.; Ma, Z. Y.; Shuai, Z. G. Toward Quantitative Prediction of Charge Mobility in Organic Semiconductors: Tunneling Enabled Hopping Model. *Adv. Mater.* **2012**, *24*, 3568−3572.

(23) Shuai, Z. G.; Wang, L. J.; Li, Q. K. Evaluation of Charge Mobility in Organic Materials: From Localized to Delocalized Descriptions at a First-Principles Level. *Adv. Mater.* **2011**, *23*, 1145−1153.

(24) Tang, L.; Long, M. Q.; Wang, D.; Shuai, Z. G. The Role of Acoustic Phonon Scattering in Charge Transport in Organic Semiconductors: A First-Principles Deformation-Potential Study. *Sci. China, Ser. B* **2009**, *52*, 1646−1652.

(25) Xi, J. Y.; Long, M. Q.; Tang, L.; Wang, D.; Shuai, Z. G. First-Principles Prediction of Charge Mobility in Carbon and Organic Nanomaterials. *Nanoscale* **2012**, *4*, 4348−4369.

(26) Adam, S.; Hwang, E. H.; Galitski, V. M.; Das Sarma, S. A Self-Consistent Theory for Graphene Transport. *Proc. Natl. Acad. Sci. U.S.A.* **2007**, *104*, 18392−18397.

(27) Zhang, Y. Y.; Pei, Q. X.; Wang, C. M. Mechanical Properties of Graphynes under Tension: A Molecular Dynamics Study. *Appl. Phys. Lett.* **2012**, *101*, 081909.